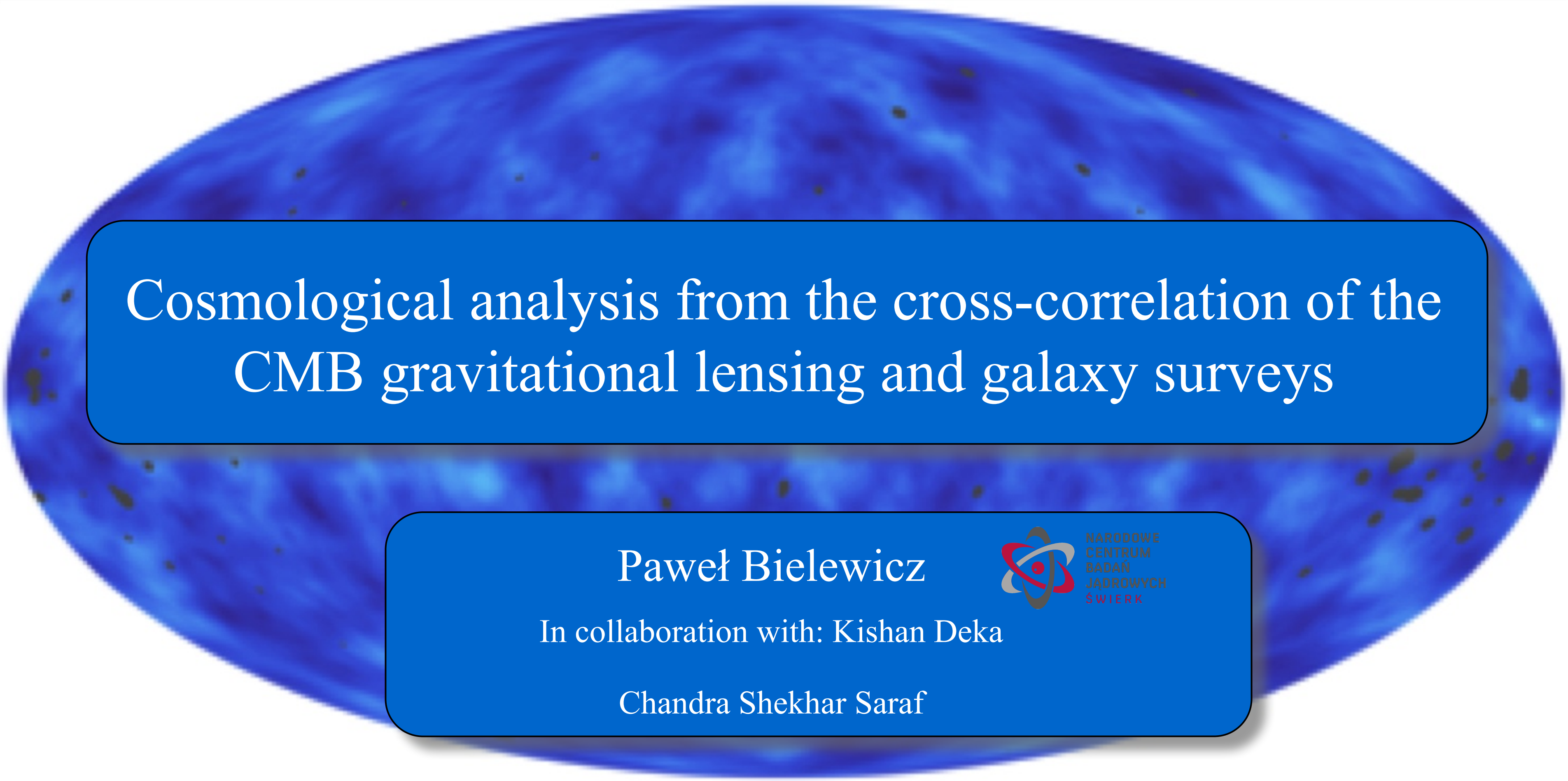

Cosmological analysis from the cross-correlation of the CMB gravitational lensing and galaxy surveys

Paweł Bielewicz

NARODOWE CENTRUM BADAŃ JĄDROWYCH ŚWIERK

In collaboration with: Kishan Deka

Chandra Shekhar Saraf

CMB gravitational lensing

- Deflection of the CMB photon paths by the large-scale structure of the Universe (~ 3’)
- Correlation of deflection angles over the sky by an angle ~ 2^{o}
- Reconstruction of lensing potential from changes in CMB anisotropy
- Lensing potential as a tracer of dark matter distribution

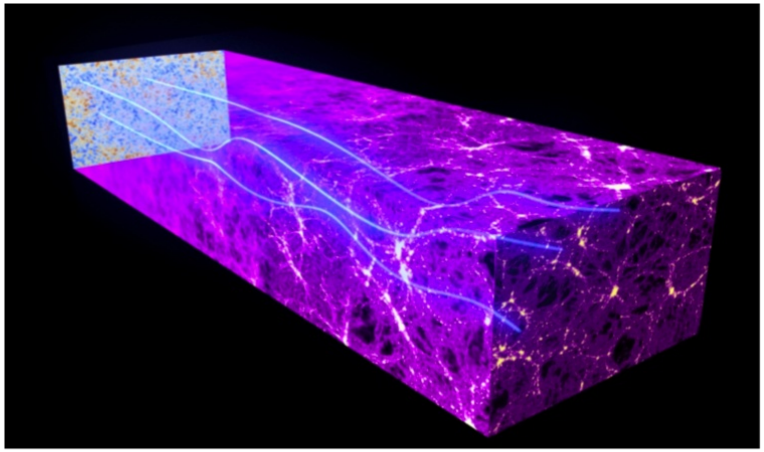

$$\phi(\hat{n}) = -\frac{2}{c^2}\int_0^{\chi_{rec}} d\chi \frac{D_{ls}}{D_l D_s}\Psi(\chi_0 - \chi, \chi\hat{n})$$

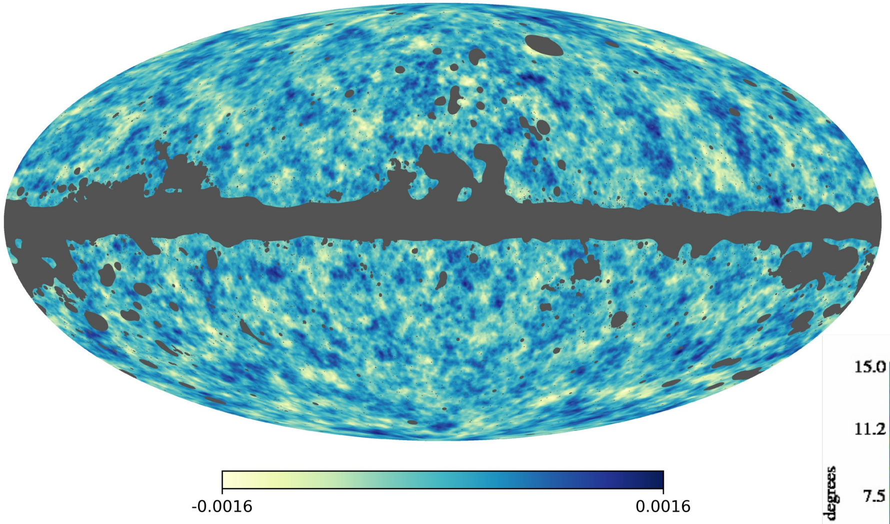

Planck collaboration et al. (2020)

$$\Delta\widetilde{T}(\hat{n}) = \Delta T(\hat{n} + \nabla\phi(\hat{n}))$$

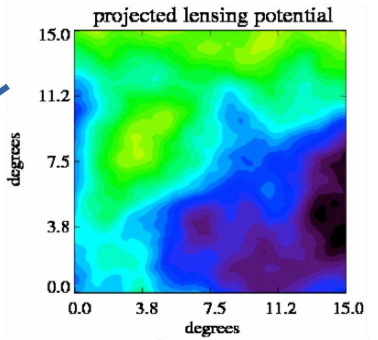

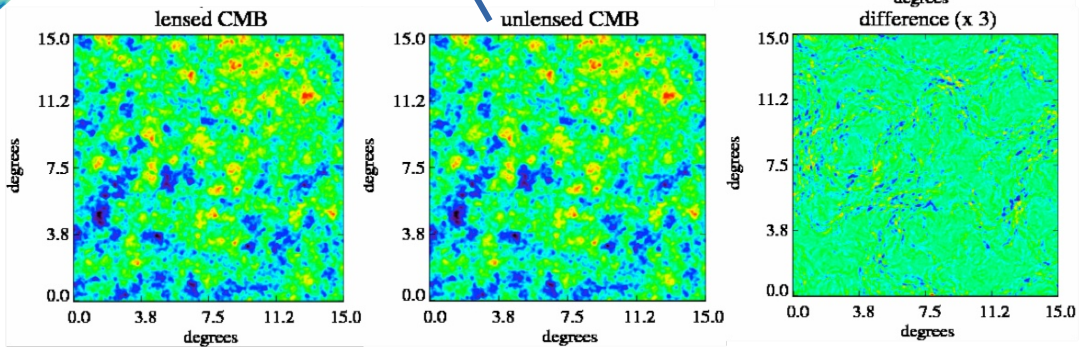

Cross-correlation between CMB lensing and galaxy surveys

- Broad CMB lensing kernel does not allow tracing time evolution of dark matter clustering

$$\phi(\hat{n}) = -\frac{2}{c^2}\int_0^{\chi_{rec}} d\chi \frac{D_{ls}}{D_l D_s}\Psi(\chi_0 - \chi, \chi\hat{n})$$

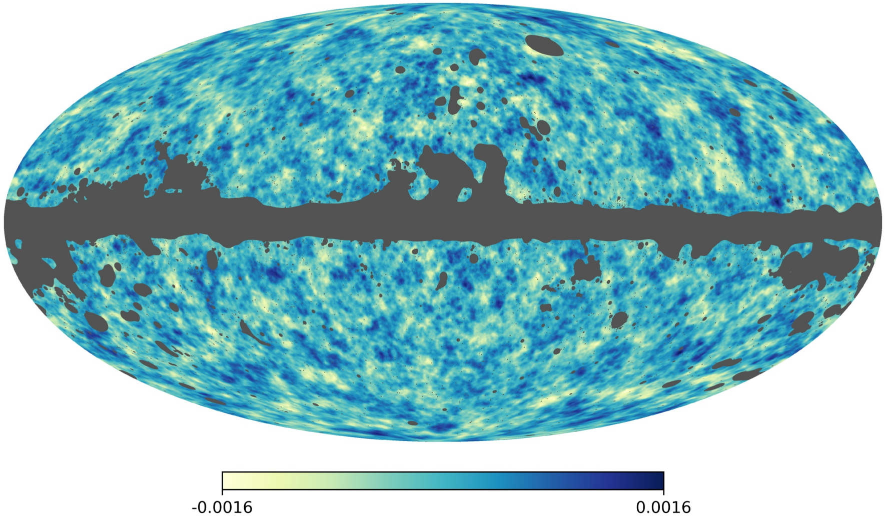

Planck collaboration et al. (2020)

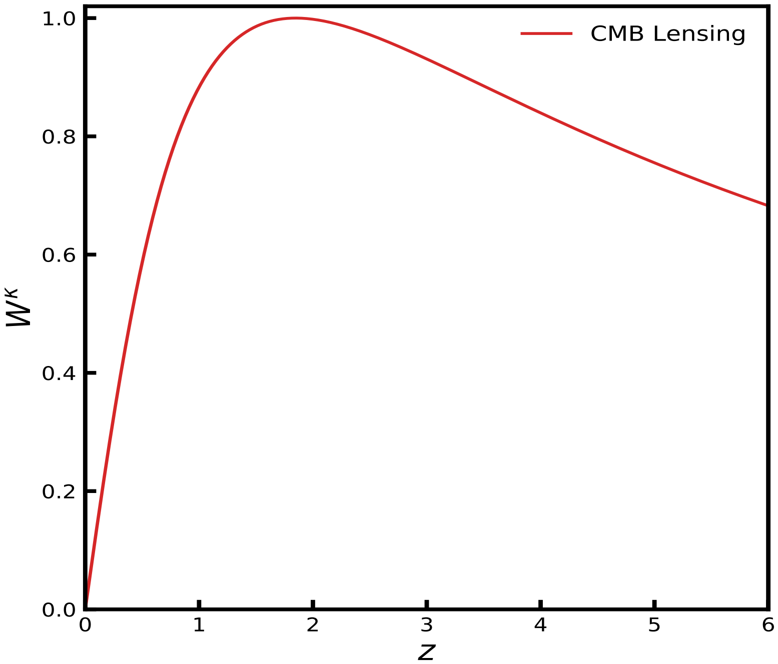

Cross-correlation between CMB lensing and galaxy surveys

- Broad CMB lensing kernel does not allow tracing time evolution of dark matter clustering
- Needed cross-correlation of CMB lensing map with objects with known redshift (galaxies, quasars, radio sources, etc.)
- Splitting redshift distribution on redshift bins (cosmic tomography: White et al. 2022; Pandey et al. 2022; Chang et al. 2022; Sun et al. 2022; Krolewski et al. 2021; Hang et al. 2021; Peacock & Bilicki 2018, Saraf et al. 2024)
- How can tomographic analysis affect delensing of CMB maps and estimation of cosmological parameters?

$$\phi(\hat{n}) = -\frac{2}{c^2}\int_0^{\chi_{rec}} d\chi \frac{D_{ls}}{D_l D_s}\Psi(\chi_0 - \chi, \chi\hat{n})$$

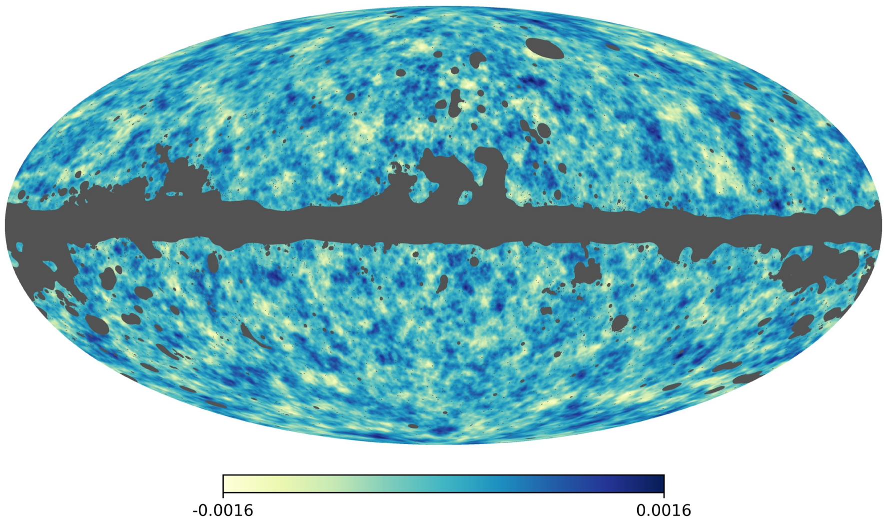

Planck collaboration et al. (2020)

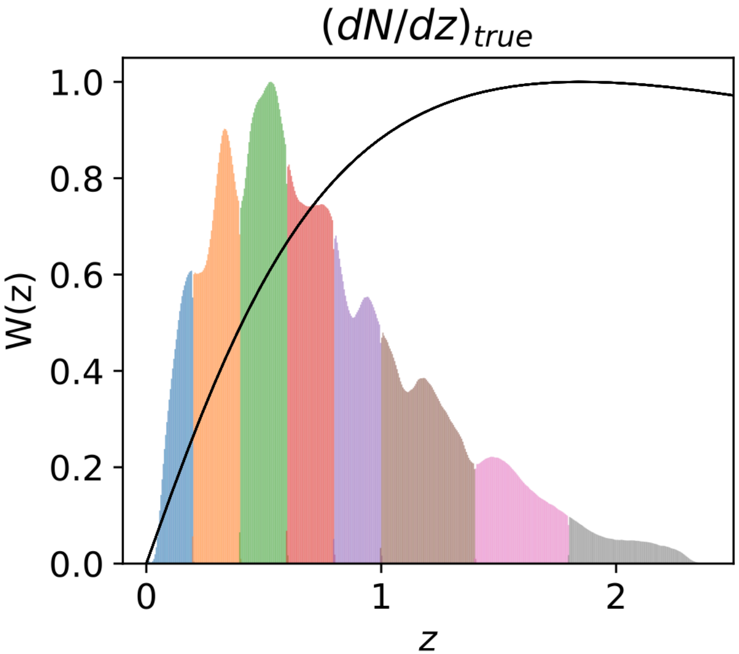

CMB gravitational lensing

- Traces evolution of the large-scale structure (constraints on dark matter, neutrino masses, etc.)
- Produces divergence-free modes (B-modes) of CMB polarisation (obstacle for detection the primordial graviatational waves)

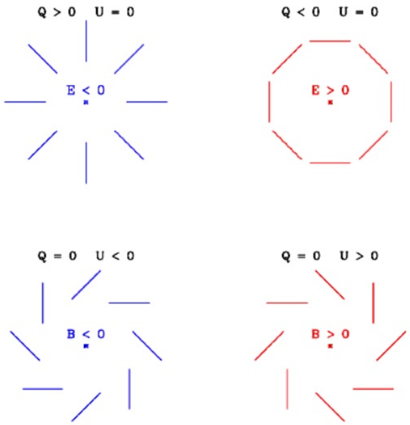

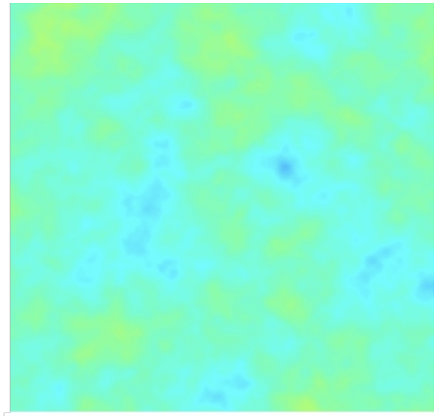
unlensed B for r=0.2 (x10)

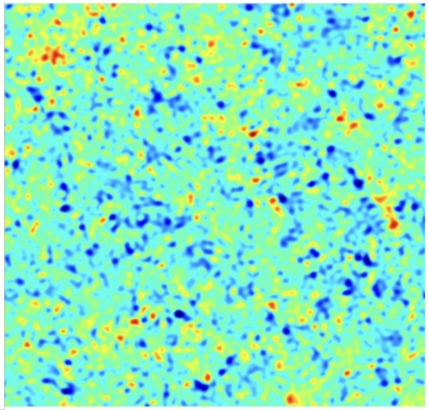
lensed B for r=0.2 (x10)

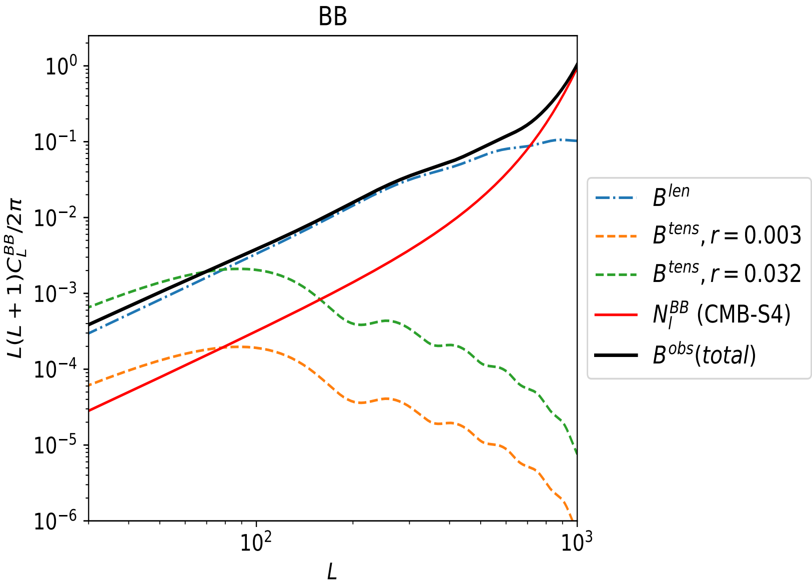

CMB gravitational lensing

- Traces evolution of the large-scale structure (constraints on dark matter, neutrino masses, etc.)
- Produces divergence-free modes (B-modes) of CMB polarisation (obstacle for detection the primordial graviatational waves)
- Delensing needed for constraining the tensor-to-scalar ratio *r*

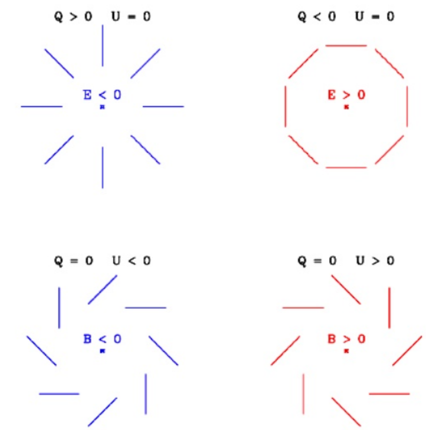

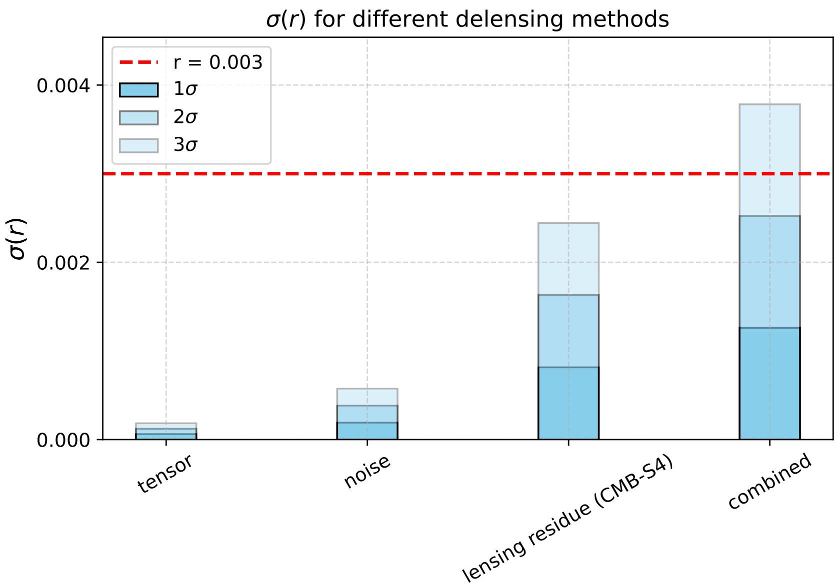

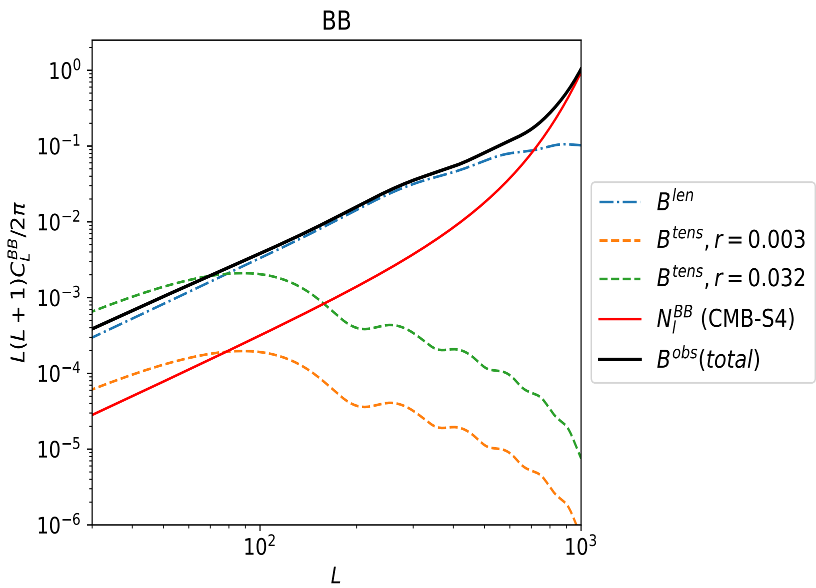

Delensing of CMB B-modes

- Distorsions of E-modes by the lensing effect generates B-modes polarisation:

$$B(\mathbf{n}) = \sum_{\ell m} a^{B}_{\ell m} \; Y_{\ell m}(\mathbf{n})$$

$$a^{B,\mathrm{lens}}_{\ell m} = \sum_{\ell' m' L M} \begin{pmatrix} \ell & \ell' & L \\ m & m' & -M \end{pmatrix} f^{EB}_{\ell\ell' L} \; a^{E}_{\ell' m'} \; \phi_{LM}$$

Delensing of CMB B-modes

- Distorsions of E-modes by the lensing effect generates B-modes polarisation:

$$B(\mathbf{n}) = \sum_{\ell m} a^B_{\ell m} \; Y_{\ell m}(\mathbf{n})$$

$$a^{B,\mathrm{lens}}_{\ell m} = \sum_{\ell' m' L M} \begin{pmatrix} \ell & \ell' & L \\ m & m' & -M \end{pmatrix} f^{EB}_{\ell\ell' L} \; a^E_{\ell' m'} \; \phi_{LM}$$

- Delensing using estimator of the lensing potential:

$$a^{B,\mathrm{temp}}_{\ell m} = \sum_{\ell' m' L M} \begin{pmatrix} \ell & \ell' & L \\ m & m' & -M \end{pmatrix} f^{EB}_{\ell\ell' L} \left(\frac{C^{EE}_{\ell'}}{C^{EE}_{\ell'} + N^{EE}_{\ell'}} a^{E,\mathrm{obs}}_{\ell' m'} \right) \left(\frac{C^{\phi\phi}_L}{C^{\phi\phi}_L + N^{\phi\phi}_L} \hat{\phi}^{EB}_{LM} \right)$$

$$a^{B,\mathrm{delens}}_{\ell m} = a^{B,\mathrm{obs}}_{\ell m} - a^{B,\mathrm{temp}}_{\ell m}$$

Delensing of CMB B-modes

- Distorsions of E-modes by the lensing effect generates B-modes polarisation:

$$B(\mathbf{n}) = \sum_{\ell m} a^B_{\ell m}\ Y_{\ell m}(\mathbf{n})$$

$$a^{B,\mathrm{lens}}_{\ell m} = \sum_{\ell' m' L M} \begin{pmatrix} \ell & \ell' & L \\ m & m' & -M \end{pmatrix} f^{EB}_{\ell\ell' L}\ a^E_{\ell' m'}\ \phi_{LM}$$

- Delensing using estimator of the lensing potential:

$$a^{B,\mathrm{temp}}_{\ell m} = \sum_{\ell' m' L M} \begin{pmatrix} \ell & \ell' & L \\ m & m' & -M \end{pmatrix} f^{EB}_{\ell\ell' L} \left(\frac{C^{EE}_{\ell'}}{C^{EE}_{\ell'} + N^{EE}_{\ell'}} a^{E,\mathrm{obs}}_{\ell' m'}\right) \left(\frac{C^{\phi\phi}_L}{C^{\phi\phi}_L + N^{\phi\phi}_L} \hat{\phi}^{EB}_{LM}\right)$$

$$a^{B,\mathrm{delens}}_{\ell m} = a^{B,\mathrm{obs}}_{\ell m} - a^{B,\mathrm{temp}}_{\ell m}$$

- Delensing using tracer of the lensing potential:

$$a^{B,\mathrm{temp}}_{\ell m} = \sum_{\ell' m' L M} \begin{pmatrix} \ell & \ell' & L \\ m & m' & -M \end{pmatrix} f^{EB}_{\ell\ell' L} \left(\frac{C^{EE}_{\ell'}}{C^{EE}_{\ell'} + N^{EE}_{\ell'}} a^{E,\mathrm{obs}}_{\ell' m'}\right) \left(\frac{C^{\phi I}_L}{C^{II}_L + N^{II}_L} I_{LM}\right)$$

Delensing of CMB B-modes

- Delensing using multiple tracers of the lensing potential:

$$I = \sum_{i,j} \left(C_{II}^{-1}\right)_{ij} C^{\phi I^j} I^i$$

$$a_{\ell m}^{B,\mathrm{temp}} = \sum_{\ell' m' LM} \begin{pmatrix} \ell & \ell' & L \\ m & m' & -M \end{pmatrix} f_{\ell\ell' L}^{EB} \left(\frac{C_{\ell'}^{EE}}{C_{\ell'}^{EE} + N_{\ell'}^{EE}} a_{\ell' m'}^{E,\mathrm{obs}}\right) \left(\frac{C_L^{\phi I}}{C_L^{II} + N_L^{II}} I_{LM}\right)$$

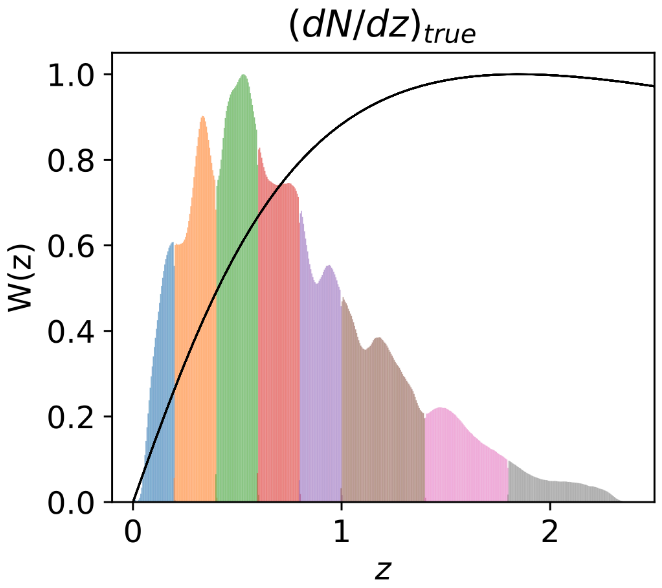

Simulations of correlated galaxy survey and CMB lensing

- Test using simulations of LSST galaxy survey
- Simulations of correlated log-normal galaxy over-density (with LSST redshift distribution estimated using the RAIL library) and CMB lensing convergence fields (consistent with CMB-S4 lensing map) using Generator for Large Scale Structure (GLASS) code (Tessore et al. 2023)

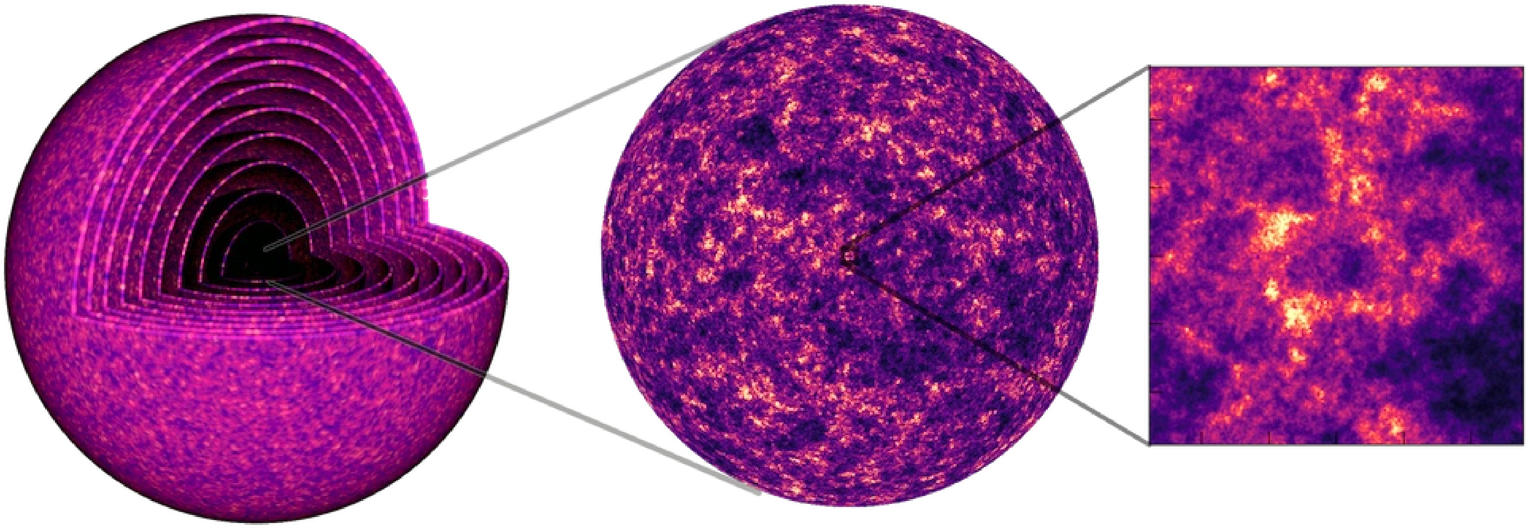

Simulations of correlated galaxy survey and CMB lensing

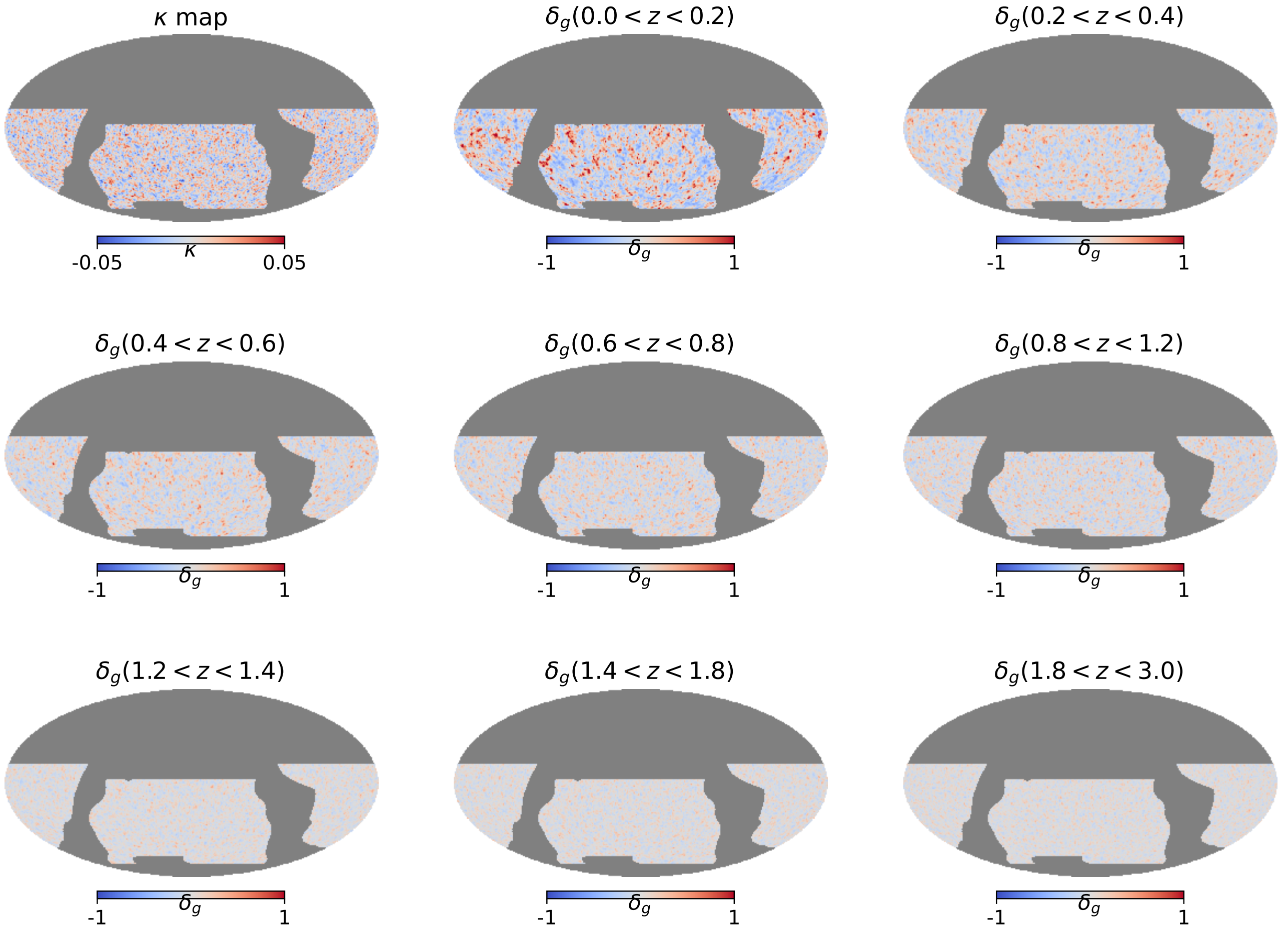

Simulations of correlated galaxy survey and CMB lensing

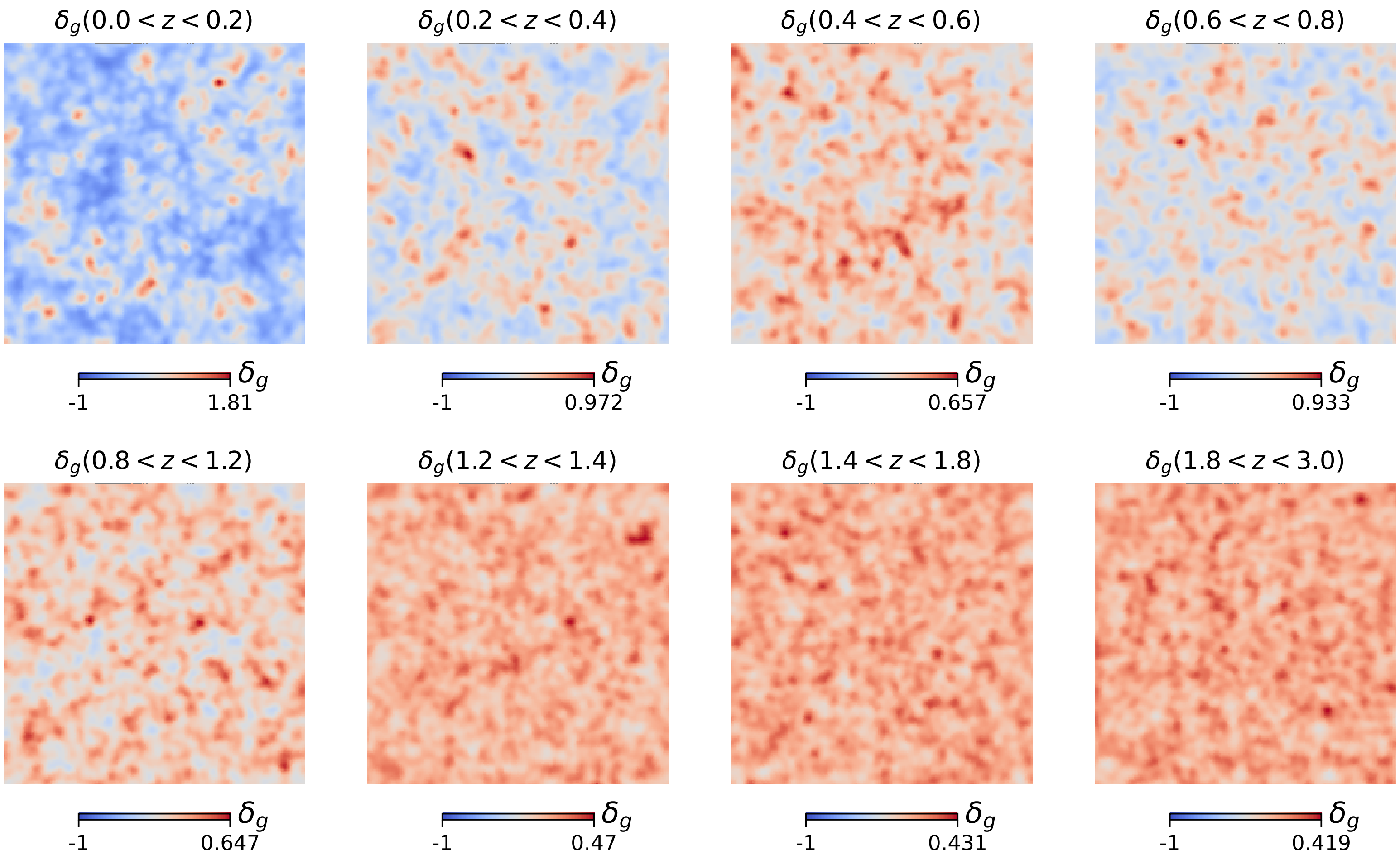

Delensing of CMB B-modes

- Estimator of the lensing potential:

$$\hat{\phi}^{XY}_{LM} = \sum_{\substack{\ell_1 m_1 \\ \ell_2 m_2}} \left[\frac{A^{XY}_L}{L(L+1)} (-1)^M \begin{pmatrix} \ell_1 & \ell_2 & L \\ m_1 & m_2 & -M \end{pmatrix} g^{XY}_{\ell_1 \ell_2 L} \right] \hat{a}^X_{\ell_1 m_1} \hat{a}^Y_{\ell_2 m_2}$$

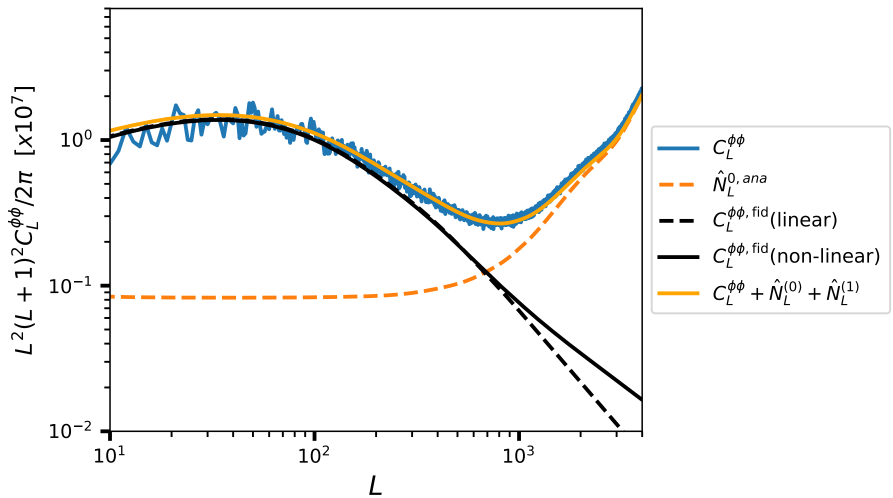

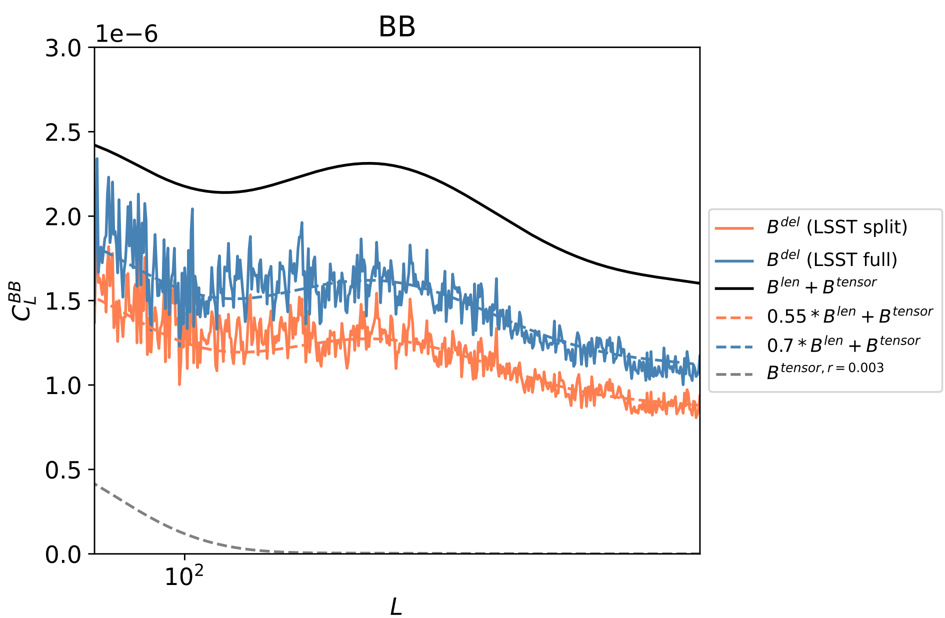

Removing up to 45% of the lensing signal from B-mode maps using LSST tomographic analysis

Delensing of CMB B-modes

- Residual power spectrum:

$$C_\ell^{B,\mathrm{res}} = \frac{1}{2\ell+1}\sum_{\ell' L} |f^{EB}_{\ell\ell' L}|^2\, C^{EE}_{\ell'}\, C^{\phi\phi}_L \left(1 - \frac{C^{EE}_{\ell'}}{C^{EE}_{\ell'} + N^{EE}_{\ell'}}\,\rho_L^2\right)$$

- Correlation coefficient (measures delensing performance):

$$\rho_\ell^2 = \sum_{i,j} \frac{C_\ell^{\phi I^i} (C_\ell^{II})^{-1}_{ij} C_\ell^{\phi I^j}}{C_\ell^{\phi\phi}}$$

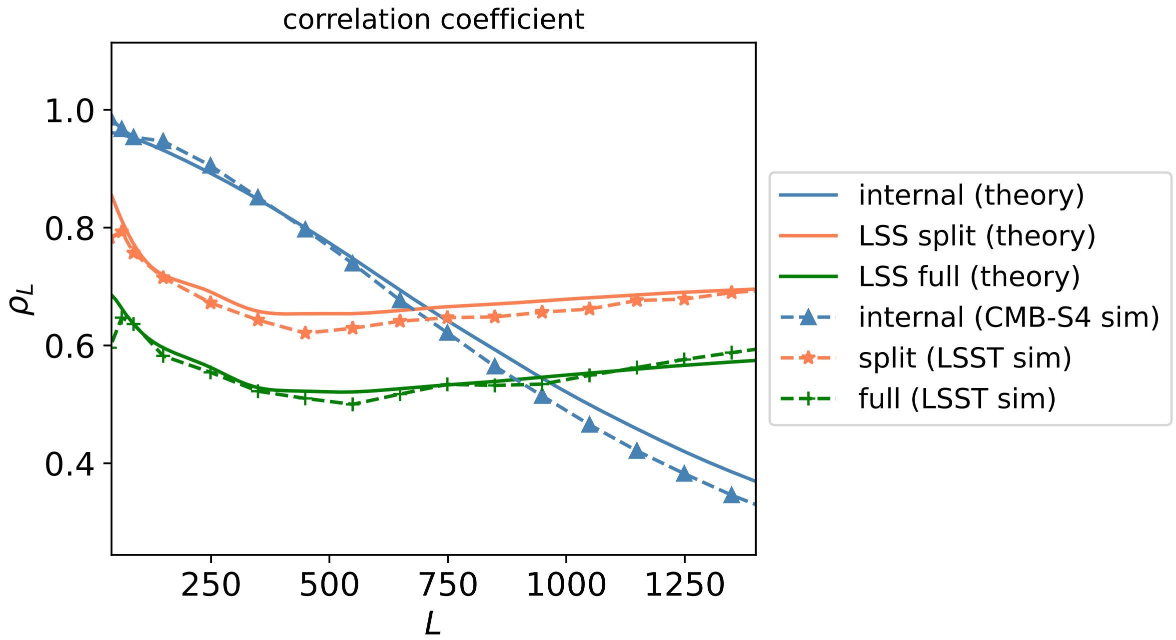

Delensing of CMB B-modes

- Delensing using combination of lensing potential tracers and internally estimated potential:

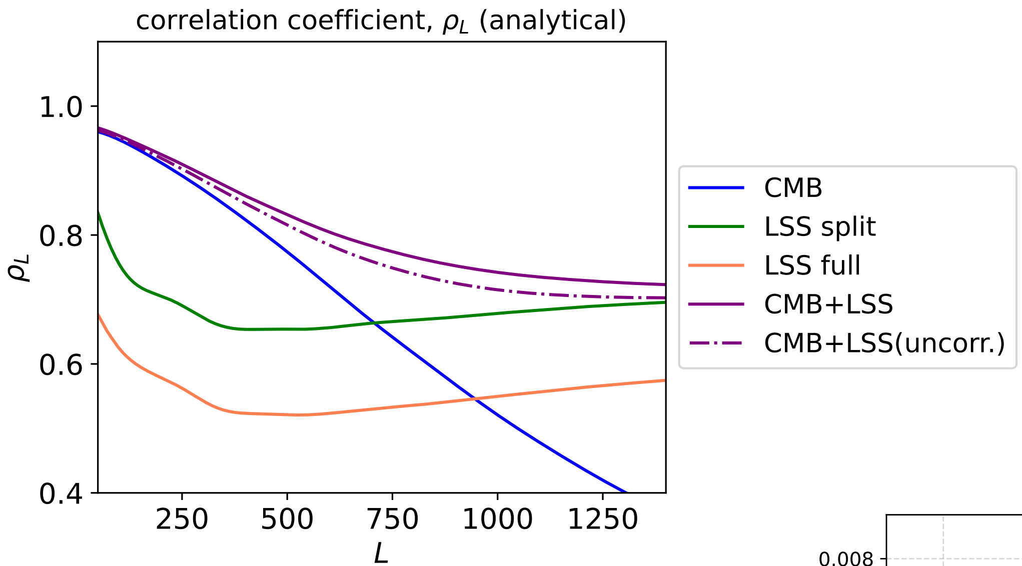

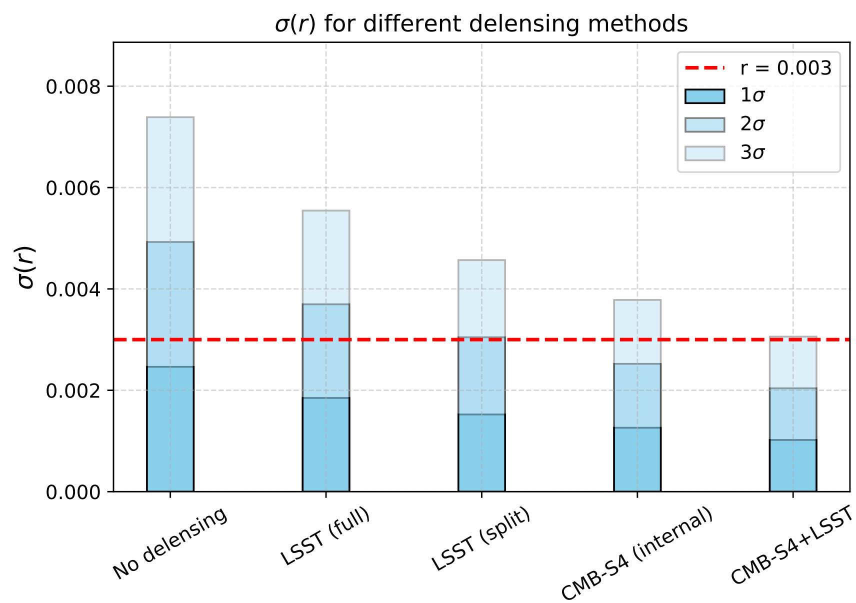

Delensing including photo-z errors

- A need of including cross-correlations between redshift bins and other systematic effects

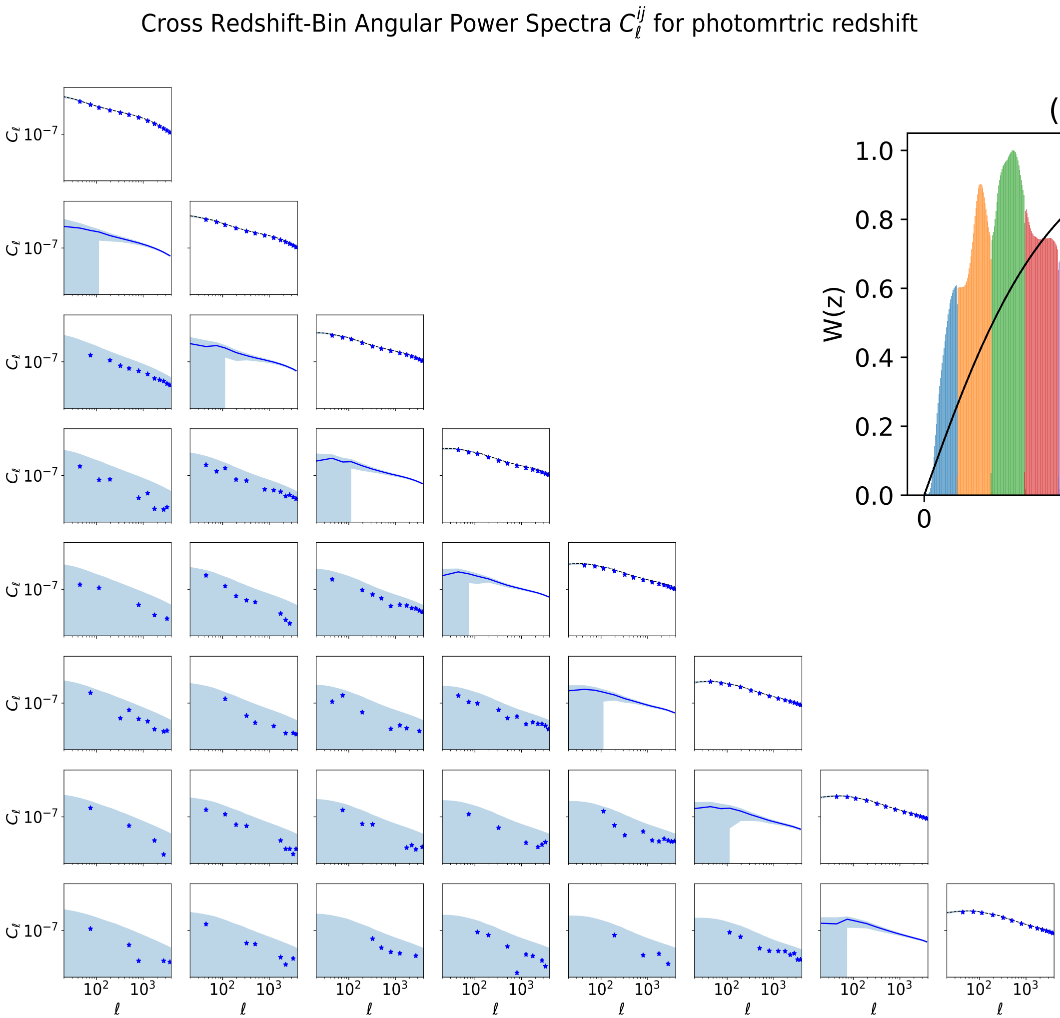

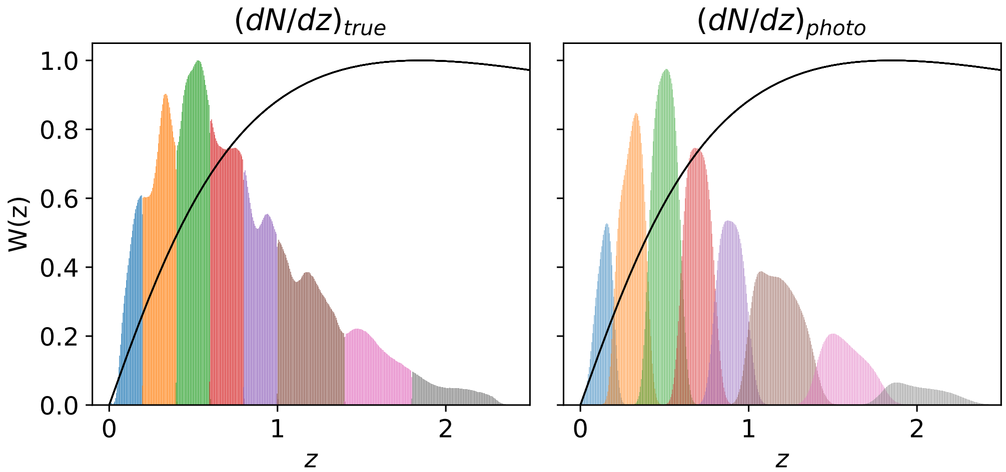

Conclusions

- Tomographic cross-correlation between CMB lensing map and LSST galaxy survey useful for improving delensing of CMB maps and constraints on the tensor-to-scalar ratio
- The most optimal combination of the multiple tracers and internally estimated lensing potential
- Needed correction for the correlation between redshift bins of galaxies and other systematic effects